

# Computing with Riemann Surfaces and Abelian Functions

General Examination

Chris Swierczewski  
University of Washington  
Department of Applied Mathematics

March 14, 2014

## Abstract

The goal of my research is to use the theory of Riemann surfaces and Abelian functions to address different application problems and to develop the software tools necessary for computing with these objects.

Abelian functions are periodic functions of  $n$  complex variables having  $2n$  independent periods. Although Abelian functions first arose in the study of Abelian integrals, they find application in many fields of mathematics such as solving non-linear integrable partial differential equations, complex algebraic geometry, optimization, and more. Algebraic curves and Riemann surfaces form a natural environment for studying these functions.

In my general examination, I will present the basic theory and algorithms involved in computing with these objects, demonstrate the implementation of these algorithms in the Python software library “abelfunctions” I developed, and present my objectives for this research.

## 1 Introduction

The Kadomtsev-Petviashvili (KP) equation is a partial differential equation used to describe the surface height of a two-dimensional periodic shallow water wave. Depending on certain physical considerations, which we will ignore, one can derive either of the following two equations

$$(-4u_t + 6uu_x + u_{xxx})_x + 3\sigma^2 u_{yy} = 0, \quad \sigma^2 = -1, \quad (1.1)$$

$$(-4u_t + 6uu_x + u_{xxx})_x + 3\sigma^2 u_{yy} = 0, \quad \sigma^2 = +1, \quad (1.2)$$

where  $u(x, y, t)$  is the surface height as a function of position  $(x, y)$  and time  $t$ . In the sequel we do not rely on this distinction and we simply refer to the *KP equation*.

The KP equation admits a large family of quasiperiodic solutions of the form

$$u(x, y, t) = 2\partial_x^2 \log \theta(Ux + Vy + Wt + z_0, \Omega) + c, \quad (1.3)$$

where  $\theta$  is the Riemann theta function.

**Definition 1.1.** *The Riemann theta function  $\theta : \mathbb{C}^g \times \mathfrak{h}_g \rightarrow \mathbb{C}$  is defined in terms of its Fourier series:*

$$\theta(z, \Omega) = \sum_{n \in \mathbb{Z}^g} e^{2\pi i \left( \frac{1}{2} n \cdot \Omega n + n \cdot z \right)}. \quad (1.4)$$

*This function converges absolutely and uniformly on compact sets in  $\mathbb{C}^g \times \mathfrak{h}_g$  where  $\mathfrak{h}_g$  is the space of all “Riemann matrices” — complex symmetric matrices with positive definite imaginary part.*

From the definition, we see that the Riemann theta function is periodic in  $z$  with integer periods and quasi-periodic in  $z$  in the columns of  $\Omega$ . In other words, if  $m, n \in \mathbb{Z}^g$  then

$$\theta(z + m + \Omega n, \Omega) = e^{-2\pi i \left( \frac{1}{2} n \cdot \Omega n + n \cdot z \right)} \theta(z, \Omega). \quad (1.5)$$

A generalization of the Riemann theta function, involving a non-integer shift in some of its arguments, is referred to as the Riemann theta function with characteristics.

**Definition 1.2.** *Let  $\alpha, \beta \in [0, 1)^g$ . The Riemann theta function with characteristic  $\begin{bmatrix} \alpha \\ \beta \end{bmatrix}$  is defined as*

$$\begin{aligned} \theta \begin{bmatrix} \alpha \\ \beta \end{bmatrix} (z, \Omega) &= \sum_{n \in \mathbb{Z}^g} e^{2\pi i \left( \frac{1}{2} (n+\alpha) \cdot \Omega (n+\alpha) + (n+\alpha) \cdot (z+\beta) \right)} \\ &= e^{2\pi i \left( \frac{1}{2} \alpha \cdot \Omega \alpha + \alpha \cdot (z+\beta) \right)} \theta(z + \Omega \alpha + \beta, \Omega). \end{aligned}$$

Note that  $\theta \begin{bmatrix} 0 \\ 0 \end{bmatrix} (z, \Omega) = \theta(z, \Omega)$ . See [4, 16, 17] for further definitions and properties of the Riemann theta function.

These solutions (1.3) are the so-called *finite genus solutions* to the KP equation and families of such solutions exist for every  $g > 0$ . In fact, the totality of solutions of this form are dense the space of all periodic solutions to KP [13]. The constants  $c \in \mathbb{C}$ ,  $U, V, W, z_0 \in \mathbb{C}^g$  and  $\Omega \in \mathfrak{h}_g$ , as well as the *genus*  $g$ , are determined from a Riemann surface. Any such Riemann surface can produce a family of solutions to KP [7]. We postpone the definition of these constants in terms of known quantities until more machinery is developed in the following sections.

In general, periodic solutions to integrable partial differential equations are *Abelian functions*.

**Definition 1.3.** An **Abelian function**  $f : \mathbb{C}^g \rightarrow \mathbb{C}$  of genus  $g \geq 1$  is a meromorphic function such that there exists  $2g$  vectors  $w_1, \dots, w_{2g} \in \mathbb{C}^g$  linearly independent over the real numbers where

$$f(z + w) = f(z),$$

for all  $z \in \mathbb{C}^g$ . When  $g = 1$  these are the elliptic functions.

Abelian functions first arose from the study of Abelian integrals

$$\int_{z_0}^{z_1} \frac{P(z, w)}{Q(z, w)} dz,$$

where  $P, Q \in \mathbb{C}[z, w]$  and  $z$  and  $w$  are related by an algebraic equation  $f(z, w) = 0$  with  $f \in \mathbb{C}[z, w]$ .

Riemann theta functions play a central role in the theory of Abelian functions in that all Abelian functions can be written as a rational function of the Riemann theta function and its derivatives (such as in the KP solution above). The primary focus of my study is the construction and numerical evaluation of these Abelian functions, particularly those arising in applications.

Abelian functions are applicable in fields other than nonlinear water waves. For example, they make explicit many computations such as those in the study of solitary waves, black hole space-times, and algebraic curves. One basic example is the calculation of bitangent lines of plane algebraic curves; these are useful for computations in optimization-related fields such as algebraic geometry and convex optimization. Bitangents can be used to represent smooth complex plane quartic curves as either a symmetric determinant of a linear form or as a sum of three squares [22]. In convex optimization, bitangents are used to construct a *visibility complex* which, in turn, is used to solve the shortest path problem in Euclidean space [24].

**Definition 1.4.** A **bitangent** to a plane algebraic curve  $C : f(x, y) = 0, f \in \mathbb{C}[x, y]$  is a line  $\mathcal{L} \subset \mathbb{C}$  that lies tangent to  $C$  at at least two distinct points.

By Bezout's Theorem, if a curve has a bitangent it necessarily must be of degree at least four [3]. A result of Plücker determines that a degree four complex curve admits exactly 28 complex bitangents [23]. In particular, Plücker showed that the number of real bitangents of any real quartic must be 28, 16, or fewer than 9. The connection between Riemann theta functions and the bitangent lines of smooth quartics was known to Riemann [2, 26] and, in fact, can be computed using the tools developed in this research. See Figure 1.1 for an example.

Finally, Riemann theta functions and algebraic curves can be used to compute linear matrix representations of algebraic curves. A theorem from classical algebraic geometry states that every homogenous polynomial  $f \in P^2 \mathbb{C}[x_0, x_1, x_2]$  can be written in the form

$$f(x_0, x_1, x_2) = \det(Ax_0 + Bx_1 + Cx_2),$$

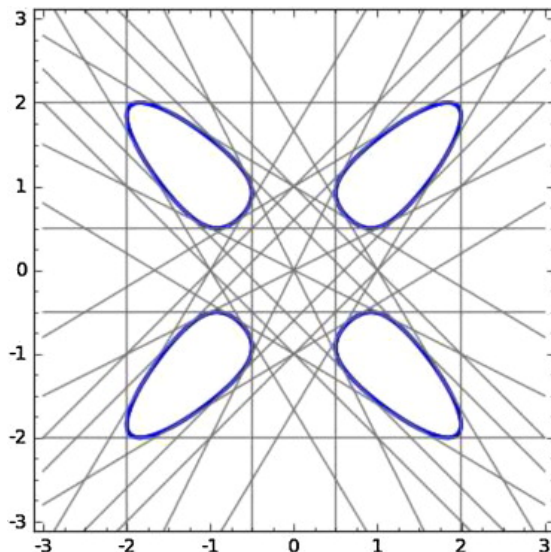


Figure 1.1: The real graph of the Edge Quartic  $C : f(x, y) = 25(x^4 + y^4 + 1) - 34(x^2y^2 + x^2 + y^2) = 0$  (in blue) and its 28 real bitangents (in grey). Note that four of them lie tangent to  $C$  at infinity. These lines were computed using the Riemann theta function.

where  $A, B, C$  are symmetric complex matrices which can be efficiently computed using Riemann theta functions. Furthermore, when the polynomial has real coefficients then  $A, B, C$  are symmetric real matrices and such representations are important in the study of spectrahedra — the solution spaces of semidefinite programs [21].

The purpose of my research is to develop efficient and performant algorithms for computing with Abelian functions on Riemann surfaces. The computational tools developed in this research program have far-reaching and varied applications.

## 2 Complex Algebraic Geometry

This section serves as a brief introduction to the theory of complex algebraic curves. Primary references are [10, 29].

### 2.1 The Projective Line

The primary motivation behind complex projective geometry is to make concrete the way in which we analyze the behavior of functions, such as polynomials, at infinity without having to resort to techniques separate from those used at finite points. For example, in applications we may need to integrate a differential along

a path on an algebraic curve going to infinity. Knowing the geometry of the curve at infinity makes such an operation computationally feasible.

In fact, anyone with an elementary complex analysis background has seen an example of projective geometry. The Riemann sphere is the complex plane  $\mathbb{C}$  with a “point at infinity” added. Let  $z$  denote the coordinate in  $\mathbb{C}$  (i.e., the point  $z = 0$  represents the origin of the complex plane). In order to discuss the point at infinity we introduce the coordinate  $w = 1/z$ . The analysis of some function at  $\infty$  is equivalent to rewriting the problem in terms of the coordinate  $w$  and examining its behavior in a neighborhood of  $w = 0$ . This explains why, for example, the exponential function

$$e^z = \sum_{n=0}^{\infty} z^n / n!,$$

though entire in the complex plane, has an essential singularity on the Riemann sphere since the exponential function in the coordinate  $w$  centered at  $w = 0$  is expressed by the series

$$\sum_{n=0}^{\infty} \frac{w^{-n}}{n!}.$$

This point at infinity is not rigorously defined because it does not make sense to *equate*  $z = \infty$ . The definition of the Riemann sphere is made explicit by the following construction: consider the set  $U = \mathbb{C}^2 - \{(0, 0)\}$ . Define the equivalence relation

$$(a_0, a_1) \sim (\lambda a_0, \lambda a_1), \quad \forall \lambda \in \mathbb{C} - \{0\}.$$

Thus two points  $(a_0, a_1)$  and  $(b_0, b_1)$  in  $U$  are considered the same if the ratios  $a_0 : a_1$  and  $b_0 : b_1$  are equal. The set of all points  $(b_0, b_1)$  equal to  $(a_0, a_1)$  is called the *equivalence class* of  $(a_0, a_1)$  and the *complex projective line*  $\mathbb{P}^1\mathbb{C}$  is the set of all such equivalence classes. That is,

$$\mathbb{P}^1\mathbb{C} := \mathbb{C}^2 / \sim.$$

The equivalence class of  $(a_0, a_1)$ , called a “point” in  $\mathbb{P}^1\mathbb{C}$ , is written  $(a_0 : a_1) \in \mathbb{P}^1\mathbb{C}$ .  $\mathbb{P}^1\mathbb{C}$  is precisely the Riemann sphere. To see this, consider the two subsets

$$U_0 = \{(a_0 : a_1) \in \mathbb{P}^1\mathbb{C} \mid a_0 \neq 0\},$$

$$U_1 = \{(a_0 : a_1) \in \mathbb{P}^1\mathbb{C} \mid a_1 \neq 0\}.$$

For any  $(a_0 : a_1) \in U_0$  we have, by the equivalence property,

$$(a_0 : a_1) = (1 : a_1/a_0) = (1 : a).$$

Similarly,  $(b_0 : b_1) = (b : 1)$  for every point in  $U_1$ . Every point in the intersection  $U_0 \cap U_1$  can be written in either of these two forms. Each of these subspaces are isomorphic to  $\mathbb{C}$  since the maps

$$\begin{aligned} \phi_0 : U_0 &\rightarrow \mathbb{C}, & \phi_0((a_0 : a_1)) &= a_1/a_0, & \text{and} \\ \phi_1 : U_1 &\rightarrow \mathbb{C}, & \phi_1((a_0 : a_1)) &= a_0/a_1, \end{aligned}$$

are continuous bijections with inverses

$$\phi_0^{-1}(a) = (1 : a), \quad (2.1)$$

$$\phi_1^{-1}(b) = (b : 1). \quad (2.2)$$

Finally, note that  $(0 : 1)$  is the only projective point in  $U_1$  which is not in  $U_0$ . Therefore, we identify  $U_0$  with the complex plane (in the coordinate  $z$ ) and the point  $P_\infty = (0 : 1)$  with the point at infinity and set

$$\mathbb{P}^1\mathbb{C} = U_0 \cup \{(0 : 1)\} \cong \mathbb{C} \cup P_\infty. \quad (2.3)$$

Indeed  $P_\infty$  is considered the point at infinity on the Riemann sphere for if one considers the image of  $(0 : 1)$  under  $\phi_0$ , though undefined since  $(0 : 1) \notin U_0$ , it maps to  $z = 1/0 = \infty$ . Again, this does not make sense without the complex projective space construction above but is merely used to illustrate the point. The coordinate transformation from  $z$  to  $w$  at the beginning of this section is equivalent to identifying  $U_1$  with the complex plane  $\mathbb{C}$  and  $\{(1 : 0)\}$  with the point at infinity, instead.

## 2.2 The Projective Plane

The natural environment we use in the sequel is not the complex projective line but the complex projective plane. In this section we construct the projective plane and examine its geometric properties. The construction is similar to that of the projective line.

Let  $U = \mathbb{C}^3 - \{(0, 0, 0)\}$ . Following the strategy of the previous section, consider the set of all ratios  $(a_0 : a_1 : a_2)$ , that is, the collection of all equivalence classes under the equivalence relation  $(a_0 : a_1 : a_2) \sim (\lambda a_0 : \lambda a_1 : \lambda a_2), \forall \lambda \in \mathbb{C} - \{0\}$ . The space of all such equivalence classes is called the two-dimensional complex projective space or *the projective plane* and is denoted  $\mathbb{P}^2\mathbb{C}$ .

Define the subsets  $U_0, U_1, U_2$  by

$$U_j = \{(a_0 : a_1 : a_2) \in \mathbb{P}^2\mathbb{C} \mid a_j \neq 0\},$$

and note that all  $(a_0 : a_1 : a_2) \in U_0$  satisfy  $(a_0 : a_1 : a_2) = (1 : a_1/a_0 : a_2/a_0)$ . We define the bijective mapping

$$\begin{aligned} \phi_0 : U_0 &\rightarrow \mathbb{C}^2, \\ \phi_0((a_0 : a_1 : a_2)) &= \left( \frac{a_1}{a_0}, \frac{a_2}{a_0} \right), \\ \phi_0^{-1}((x, y)) &= (1 : x : y). \end{aligned}$$

The mappings  $\phi_1$  and  $\phi_2$  are similarly defined on  $U_1$  and  $U_2$ , respectively. Therefore, we can identify  $U_0$  with the complex plane  $\mathbb{C}^2$ .

Consider the space  $U_0^c = \mathbb{P}^2\mathbb{C} - U_0$ . By definition, every point in  $U_0^c$  is of the form  $(0 : a_1 : a_2)$ . By definition, every point in  $U_0^c$  determines a point on

the complex projective line  $P^1\mathbb{C}$ . The converse is true as well, resulting in the bijection

$$(0 : a_1 : a_2) \in P^2\mathbb{C} \leftrightarrow (a_1 : a_2) \in P^1\mathbb{C}.$$

By identifying  $U_0^c$  with  $P^1\mathbb{C}$  we may write

$$P^2\mathbb{C} = U_0 \cup U_0^c \cong \mathbb{C}^2 \cup P^1\mathbb{C} \quad (2.4)$$

where  $U_0^c \cong P^1\mathbb{C}$  is called the *line at infinity*, denoted  $l_\infty$ , and  $U_0 \cong \mathbb{C}^2$  is called the *complex affine plane*. We may also identify the complex affine plane with the sets  $U_1$  or  $U_2$  and the line at infinity with their complements.

We saw a natural geometric interpretation of  $P^1\mathbb{C}$  in the previous section. Does such an interpretation exist for  $P^2\mathbb{C}$ ? Consider a line in the complex affine plane  $\mathbb{C}^2$  which can be written in the form

$$\alpha + \beta x + \gamma y = 0, \quad \text{where } (\beta, \gamma) \neq 0, \alpha, \beta, \gamma \in \mathbb{C}.$$

Using the inverse mapping  $\phi_0^{-1}$  on  $\mathbb{C}^2$  we have

$$x = \frac{x_1}{x_0} \text{ and } y = \frac{x_2}{x_0},$$

where  $(x_0 : x_1 : x_2)$  are the coordinates of  $P^2\mathbb{C}$ , and we get the line

$$\alpha x_0 + \beta x_1 + \gamma x_2 = 0.$$

This equation, called the *homogenization* of the affine curve, makes sense in all of  $P^2\mathbb{C}$ . Setting  $x_0 = 1$  gives the original affine line. On the other hand, setting  $x_0 = 0$  gives the equation

$$\beta x_1 + \gamma x_2 = 0,$$

which is the equation of the line in  $l_\infty$ . However, this implies  $x_1/x_2 = -\gamma/\beta$ . Hence the projective point  $(0 : -\gamma : \beta)$  satisfies the equation

$$\alpha x_0 + \beta x_1 + \gamma x_2 = 0$$

and is, in fact, the only projective point in  $l_\infty$  on the line.

This means that the line “intersects”  $l_\infty$  at the point  $(0 : -\gamma : \beta)$  and that this intersection point depends only on the slope of the affine portion of the line. Hence, the line at infinity has the geometric meaning that each point on it is the intersection point of an entire family of parallel lines in  $\mathbb{C}^2$ . This leads to a generalization of a theorem from classical planar geometry: *any two, distinct lines in  $P^2\mathbb{C}$  intersect at exactly one point.*

## 2.3 Projective Plane Curves

The set of all points  $(x_0, x_1, x_2)$  satisfying

$$\alpha x_0 + \beta x_1 + \gamma x_2 = 0$$

is called a projective line and is a simple example of a projective algebraic curve (of degree one). In this section we introduce various properties of general projective curves.

An *complex plane algebraic curve* is the zero locus of the homogenization of a polynomial  $f \in \mathbb{C}[x, y]$ . That is, given a polynomial  $f(x, y) = \alpha_n(x)y^n + \alpha_{n-1}(x)y^{n-1} + \cdots + \alpha_0(x)$  its homogenization is the polynomial  $F \in \mathbb{P}^2\mathbb{C}[x_0, x_1, x_2]$  where

$$F(x_0, x_1, x_2) = x_0^d f(x_1/x_0, x_2/x_0).$$

where  $d$  is the degree of  $F$ . The homogeneity of  $F$  means that we can write

$$F(x_0, x_1, x_2) = \sum_{i+j+k=d} \alpha_{ijk} x_0^i x_1^j x_2^k.$$

In terms of the projective polynomial  $F$ , its affine part can be written  $f(x, y) = F(1, x, y)$ . As in the case of a projective line,  $f$  can be thought of as a projection of the polynomial  $F$  onto  $\mathbb{C}^2$  and there is always a one-to-one correspondence between an affine polynomial and its homogenization. Therefore, a *complex plane algebraic curve* is the set

$$C = \{(x_0 : x_1 : x_2) \in \mathbb{P}^2\mathbb{C} : F(x_0, x_1, x_2) = 0\}.$$

Important to the study of projective curves, and specifically in the computational work described here, are singular points.

**Definition 2.1.** A point  $a = (a_0 : a_1 : a_2) \in C$  is a **singular point of  $C$** , or a *multiple point of  $C$* , if

$$\left( \frac{\partial F}{\partial x_0}, \frac{\partial F}{\partial x_1}, \frac{\partial F}{\partial x_2} \right) (a) = (0, 0, 0).$$

Consider the case when  $a = (1 : 0 : 0)$  (corresponding to the point  $(0, 0)$  in the affine plane  $\mathbb{C}^2$ ) is a singular point of  $F$ . The affine portion of the curve is

$$f(x, y) = \sum_{i+j \geq 2} c_{ij} x^i y^j.$$

Note that the constant term is zero since  $(0, 0)$  is a point on the affine curve and the linear term vanishes since  $(0, 0)$  is a singular point. We write

$$f(x, y) = f_m(x, y) + f_{m+1}(x, y) + \cdots + f_d(x, y), \quad m \geq 2,$$

where each  $f_n$  is the sum of all terms of  $f$  of degree  $n$ ; that is, terms of the form  $c_{ij} x^i y^j$  such that  $i + j = n$ . The smallest such  $m$  with non-zero term  $f_m$  appearing in  $f$  is called the *multiplicity* of the singular point  $(1 : 0 : 0)$ . Singularities with multiplicity two are called *double points*, those with multiplicity three are called *triple points*, and so on.

The homogeneous term  $f_m$  can be factored into linear factors

$$f_m(x, y) = \prod_{j=1}^m (\alpha_j x - \beta_j y).$$

We call the space  $f_m(x, y) = 0$  the *tangent cone of the plane curve  $C$*  at  $a = (1 : 0 : 0)$  consisting of a finite number of intersecting lines  $L_j : \alpha_j x - \beta_j y$ .

When a generic affine point  $a = (1 : c : d)$  is a singular point we write the affine curve in the form

$$f(x, y) = \sum_{i+j \geq 2}^d \tilde{c}_{ij} (x - c)^i (y - d)^j$$

which we can write as a sum of polynomials  $g_n(x - c, y - d)$  homogenous in  $x - c$  and  $y - d$ .

In the case when the singular point  $a = (0 : 1 : b) \in l_\infty$  we repeat the above process with the affine curve

$$g(u, v) = \frac{1}{x_1^d} F(x_0, x_1, x_2) = F(u, 1, v), \quad u = \frac{x_0}{x_1}, v = \frac{x_2}{x_1},$$

which is a projection of  $F$  onto  $U_1 \cong \mathbb{C}$  instead of  $U_0$ . We write  $g$  as a sum of terms of the form  $g_{ij} u^i (v - b)^j$ . Finally, in the case  $a = (0 : 0 : 1) \in l_\infty$  we use the affine curve

$$h(w, z) = \frac{1}{x_2^d} F(x_0, x_1, x_2) = F(w, z, 1), \quad w = \frac{x_0}{x_2}, z = \frac{x_1}{x_2},$$

and write  $h$  as a sum of terms of the form  $h_{ij} w^i z^j$ .

**Example 2.2.** Consider the cubic curve

$$C : F(x_0, x_1, x_2) = x_0^4 x_2^3 + 2x_0^3 x_1^3 x_2 - x_1^7$$

In complex affine space  $x_0 = 1$  this curve is

$$f(x, y) = F(1, x, y) = y^3 + 2x^3 y - x^7.$$

A plot of  $f$  for  $x, y$  real is shown in Figure 2.1. For  $a = (a_0 : a_1 : a_2)$  we have

$$\begin{aligned} \frac{\partial F}{\partial x_0}(a) &= 4a_0^3 a_2^3 + 6a_0^2 a_1^3 a_2, \\ \frac{\partial F}{\partial x_1}(a) &= 6a_0^3 a_1^2 a_2 - 7a_1^6, \\ \frac{\partial F}{\partial x_2}(a) &= 3a_0^4 a_2^2 + 2a_0^3 a_1^3. \end{aligned} \tag{2.5}$$

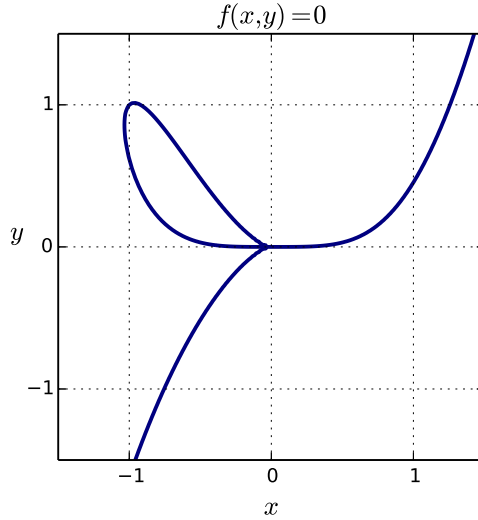


Figure 2.1: A real plot of the curve  $C : f(x, y) = y^3 + 2x^3y - x^7$ . The plot suggests that  $(x_0 : x_1 : x_2) = (1 : 0 : 0)$ , corresponding to  $(x, y) = (0, 0)$ , is a singular point of  $C$ .

First, we find the finite singular points of  $C$ . Setting  $a_0 = 1$  and solving the above equations for  $a_1$  and  $a_2$  we see that  $p = (1 : 0 : 0)$  is the only finite singular point of  $F$ . Note that

$$f(x, y) = f_3(x, y) + f_4(x, y) + f_7(x, y),$$

$$f_3(x, y) = y^3, \quad f_4(x, y) = 2x^3y, \quad f_7(x, y) = -x^7,$$

and that  $f_3$ ,  $f_4$ , and  $f_7$  are homogeneous of degrees 3, 4, and 7, respectively. Therefore,  $p$  is a singular point of multiplicity 3 with

$$f_3(x, y) = y^3 = 0,$$

as the equation for the tangent cone at  $p$ . These properties are suggested by Figure 2.1 where, near the point  $p$ , the real curve looks like the intersection of three curves well approximated by the line  $y = 0$  near the point  $x = 0$ .

Setting  $a_0 = 0$ , the only expression in Equation (2.5) that does not reduce to zero is

$$\frac{\partial F}{\partial x_1}((0, a_1, a_2)) = -7a_1^6 = 0,$$

implying that the point  $a = (0 : 0 : 1)$  is the only singular point at infinity. The curve at infinity centered at  $(0 : 0 : 1)$  is

$$h(w, z) = F(w, z, 1) = w^4 + 2w^3z^3 - z^7.$$

The order of this singularity is four since this is the degree of the lowest degree homogeneous term. The tangent cone at  $a$  is  $g_4(w, z) = w^4$ .

## 2.4 Connection to Riemann Surfaces

There is a close relationship between the study of compact Riemann surfaces and that of algebraic curves. Recall that a Riemann surface  $X$  is a complex manifold of complex dimension one endowed with an *atlas*: an open covering  $\{U_\alpha\}_{\alpha \in A}$  of  $X$  together with a collection of homeomorphisms  $\{z_\alpha : U_\alpha \rightarrow \mathbb{C}\}_{\alpha \in A}$ , called *local parameters*, such that every pair of *transition functions*

$$f_{\beta, \alpha} := z_\beta \circ z_\alpha^{-1} : z_\alpha(U_\alpha \cap U_\beta) \rightarrow z_\beta(U_\alpha \cap U_\beta),$$

is holomorphic. The pairs  $(U_\alpha, z_\alpha)$  are called *coordinate charts*. In other words, a Riemann surface is a topological space such that for all  $P \in X$  there is a neighborhood of  $P$  homeomorphic to an open subset of the complex plane and one can analytically continue from any  $P \in X$  to any  $Q \in X$  via transition functions.

The Riemann sphere  $X = \mathbb{C}^*$  is an example of a Riemann surface. Its atlas consists of two coordinate charts  $(U_1, z_1)$  and  $(U_2, z_2)$  with

$$\begin{aligned} U_1 &= \mathbb{C}, & z_1 &= z, \\ U_2 &= (\mathbb{C} - \{0\}) \cup \{\infty\}, & z_2 &= 1/z. \end{aligned}$$

This is a valid atlas since the transition functions

$$\begin{aligned} f_{1,2}, f_{2,1} &: (\mathbb{C} - \{0\}) \rightarrow (\mathbb{C} - \{0\}) \\ f_{1,2} &= z_1 \circ z_2^{-1} = 1/z \\ f_{2,1} &= z_2 \circ z_1^{-1} = 1/z \end{aligned}$$

are holomorphic on  $U_1 \cap U_2 = \mathbb{C} - \{0\}$ .

These relationships between curves and Riemann surfaces are embodied by the following two theorems [10].

**Theorem 2.3. (Normalization Theorem.)** *For any irreducible algebraic curve  $C \subset \mathbb{P}^2\mathbb{C}$  there exists a compact Riemann surface  $X$  and a holomorphic mapping*

$$\sigma : X \rightarrow \mathbb{P}^2\mathbb{C},$$

*such that  $\sigma(X) = C$  and  $\sigma$  is injective on the inverse image of the set of smooth points of  $C$ .*

A Riemann surface together with the mapping  $\sigma$  is called the *normalization of  $C$* . Loosely speaking, the normalization theorem states that an algebraic curve is a Riemann surface except at the singular points.

Conversely, every compact Riemann surface can be represented by an algebraic curve.

**Theorem 2.4.** *Any compact Riemann surface  $X$  can be obtained through the normalization of a certain plane algebraic curve  $C$  with at most ordinary double points. That is, there exists a holomorphic mapping*

$$\sigma : X \rightarrow \mathbb{P}^2\mathbb{C}$$

*such that  $\sigma(X)$  is an algebraic curve possessing at most ordinary double points.*

Many of the geometric algorithms presented in this document are designed to avoid singular points. Except, for example, when we want to integrate a 1-form along a path leading to a singular point in which case we “unwrap” the singularity using Puiseux series. This is discussed in more detail in the following section. However, because of this we use the terms “curve” and “Riemann surface” interchangeably.

Additionally, the algorithms presented in this document primarily work with the affine part  $f(x, y)$  of the curve  $F(x_0, x_1, x_2)$ . If analysis on the line at infinity is necessary, for example, when computing the singular points of a curve, we consider an affine projection  $g$  of  $F$  onto  $l_\infty$ ,

$$g(u, y) = u^d f(1/u, y) = 0.$$

Thus, the surface considered here is the branched algebraic  $y$ -covering of the complex  $x$ -Riemann sphere, the set of all  $(x, y)$ -solutions to the affine polynomial equation

$$C = \{(x, y) \in \mathbb{C} \mid f(x, y) = \alpha_d(x)y^d + \alpha_{d-1}(x)y^{d-1} + \cdots + \alpha_1(x)y + \alpha_0(x) = 0\},$$

as  $x$  varies along all of  $\mathbb{C}$ . We treat  $x$  and  $y$  as the independent and dependent variables of the equation, respectively.

A point  $\alpha \in \mathbb{C}$  is called a *regular point* of  $C$  if

$$f(\alpha, y) = 0$$

has  $d$  distinct  $y$ -roots  $y_0, \dots, y_{d-1}$ . A point  $\alpha \in \mathbb{C}$  is called a *discriminant point* if it is not regular. The point  $\alpha = \infty$  is a regular point of  $C$  if

$$g(0, y)$$

has  $d$  distinct roots.

A *place*  $P$  is an element of  $X$ . For all but finitely many places,  $P$  is given by a pair  $(\alpha, \beta)$  such that  $f(\alpha, \beta) = 0$ . However, some places, particularly those where  $\alpha$  is a discriminant point, instead needs to be represented by a pair of series  $(x(t), y(t))$  in some local coordinate  $t$ . This will be discussed in more detail in the following section.

### 3 Computing Period Matrices

This section introduces the concepts and algorithms needed to compute period matrices of Riemann surfaces. Each subsection examines a major concept behind this calculation and provides a theoretical overview of the component, a

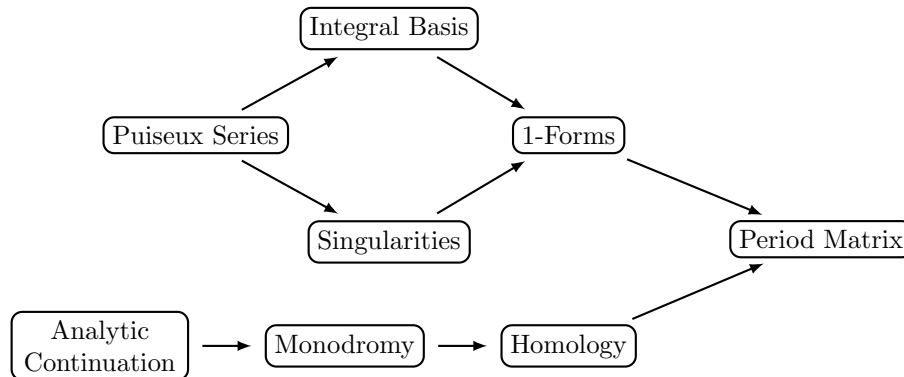


Figure 3.1: The major computations performed by `abelfunctions` and their dependencies on one another.

brief description of the algorithm used to compute the component, and examples presented in Python using the software library `abelfunctions`.

Please note that `abelfunctions`, though largely functional, is still in early stages of development. Therefore, the library syntax presented in this document may not match the syntax of future versions. Consult the documentation located at [www.cswiercz.info/abelfunctions](http://www.cswiercz.info/abelfunctions) for up to date information on the package.

The two primary ingredients involved in computing period matrices are a *basis of closed cycles* on a Riemann surface  $X$  and a *basis of holomorphic differentials* on  $X$ . Both of these depend on the components discussed in this section. The dependency relationship of all of these components is outlined in Figure 3.1, which forms the outline of this section. The book chapter [5] serves as a primary reference for this section.

### 3.1 Puiseux Series

#### Theory

Every analytic function  $f = f(x)$  admits a local Taylor series representation in a neighborhood about  $x = \alpha$ . If the function is meromorphic it still admits a local series representation in the form of a Laurent series. An extension of Taylor series are the Laurent series

$$f(x) = \sum_{n=N}^{\infty} c_n (x - \alpha)^n$$

for some  $N \in \mathbb{Z} \cup \{-\infty\}$  depending on  $\alpha$ . In both of these situations the variable  $x$  is a *local coordinate* of  $f$  near the point  $\alpha$ .

For algebraic curves, local coordinates are given in terms of Puiseux series, which can be thought of as an extension of Laurent series.

**Definition 3.1.** A **Puiseux series expansion** of a curve  $C : f(x, y) = 0$  at the point  $x = \alpha$  is a collection of  $j = 1, \dots, m \leq d = \deg_y f$  series of the form

$$P_j(t) = \begin{cases} x_j(t) = \alpha + \lambda_j t^{e_j}, \\ y_j(t) = \sum_{k=N}^{\infty} \beta_{jk} t^{n_{jk}}, \end{cases}$$

where  $N \in \mathbb{Z} \cup \{-\infty\}$ ,  $\alpha, \lambda_j, \beta_{jk} \in \mathbb{C}$ , and  $e_j, n_{jk} \in \mathbb{Z}$ . Each Puiseux series  $P_j$  is a “place” on  $C$ .

A place  $P_j = P_j(t)$  satisfies

$$f(P_j(t)) := f(x_j(t), y_j(t)) = 0.$$

When a Puiseux series  $P_j(t)$  represents an expansion about a non-singular  $(\alpha, \beta_j)$  on the curve then  $P(0) = (\alpha, \beta)$ . This is not necessarily the case about singular places. We list some additional important facts and properties of Puiseux series.

- The integer  $|e_j|$  is called the *branching number* or *ramification index* of the series expansion at that place:  $|e_j| > 1$  when  $x = \alpha$  is a branch point of the curve.
- The number of Puiseux series  $m$  at a branch point  $x = \alpha$  is strictly less than  $d = \deg_y f$ . However,  $d = \sum_{j=1}^m |e_j|$ .
- The field of Puiseux series is a splitting field for  $\mathbb{C}[x, y] = \mathbb{C}[x][y]$ . That is, given any  $f \in \mathbb{C}[x, y]$  and Puiseux series expansions about any  $x = \alpha$  we can write

$$f(x, y) = \prod_{j=1}^m \prod_{k=1}^{e_j} \left( y - y_j \left( (e/\lambda_j)^{2\pi i k / e_j} (x - \alpha) \right) \right),$$

where the first product ranges over all Puiseux series  $P_j$  at  $x = \alpha$  and the second product ranges over all  $y$ -components  $y_j(x_j)$  when solving for  $t$  in terms of  $x$ . Note that a Puiseux series  $P_j$  with ramification index  $|e_j| > 1$  splits into  $|e_j|$   $y$ -series in  $x$ .

### Algorithm

The algorithm used in *abelfunctions* for computing truncations of Puiseux series expansions is based on that of Duval [8]. The main ingredient of the algorithm are Newton polygons of algebraic curves. We give a brief outline of the process here.

- The goal of the algorithm is to compute a list of tuples  $\pi = (\tau_1, \tau_2, \dots, \tau_R)$  where  $\tau_i = (q_i, \mu_i, m_i, \beta_i, \eta_i)$ . These tuples define the relations

$$\begin{aligned} X_{i-1} &= \mu_i X_i^{q_i}, \\ Y_{i-1} &= (\beta_i + \eta_i Y_i) X_i^{m_i}, \end{aligned}$$

where  $i = 1, \dots, R$ . To obtain the desired Puiseux series we set  $x = X_0$ ,  $y = Y_0$ , and  $t = X_R$  and eliminate the intermediate variables  $X_1, \dots, X_{R-1}$  and  $Y_1, \dots, Y_{R-1}$ .

- The first set of  $\tau_i$  computed are those representing the *singular part* of  $P$ , that is, the part of the series if the Puiseux series has a ramification index  $|e_j| > 1$ . This is done using the Newton polygon method. The output of this stage of the algorithm provides enough information to distinguish the Puiseux series expansions at  $x = \alpha$ .
- Finally the algorithm computes the *regular* terms of the Puiseux series using a standard Taylor series techniques.

## Examples

**Example 3.2.** Consider the curve

$$C : f(x, y) = y^3 + 2x^3y - x^7 = 0.$$

As seen in Example 2.2, the point  $(x, y) = (0, 0)$  is a singular point of  $C$ . The Puiseux series expansions lying above  $x = 0$  are all of the form

$$P_1(t) = \begin{cases} x(t) = t, \\ y(t) = \frac{t^4}{2} - \frac{t^9}{16} + \frac{3t^{14}}{128} + \dots, \end{cases}$$

$$P_2(t) = \begin{cases} x(t) = -\frac{t^2}{2}, \\ y(t) = -\frac{t^3}{2} - \frac{t^8}{64} + \frac{3t^{13}}{4096} + \dots. \end{cases}$$

We compute these expansions using `abelfunctions`.

```

1  from abelfunctions import *
2  from sympy.abc import x,y,t
3
4  f = y**3 + 2*x**3*y - x**7
5  alpha = 0
6
7  P = puiseux(f, x, y, alpha, nterms=3, parametric=t)
8
9  print 'Puiseux Expansions at x = %s:'%(alpha)
10 for Pj in P:
11     sympy.pprint(Pj)
12     print

```

---

```

Puiseux Expansions at x = 0:
      14      9      4
      3*t      t      t
(t, ----- - -- + --)
      128     16     2

```

2	13	8	3
-t	3*t	t	t
(----	-----	- - - -	----
2	4096	64	2

MORE EXAMPLES WILL BE INSERTED HERE.

### 3.2 Singularities

#### Theory

Recall from Definition 2.1 that a point  $a$  on a projective curve  $C$  is a singular point if

$$\left( \frac{\partial F}{\partial x_0}, \frac{\partial F}{\partial x_1}, \frac{\partial F}{\partial x_2} \right) (a) = (0, 0, 0).$$

For singular points of the form  $a = (1 : \alpha, \beta)$ , this is equivalent to

$$\frac{\partial f}{\partial x}(\alpha, \beta) = 0, \quad \frac{\partial f}{\partial y}(\alpha, \beta) = 0,$$

where  $f$  is the affine portion of the curve. The singular points of a curve need to be determined not only for the numerical analytic continuation and integration methods discussed below, so we can appropriately desingularize the curve  $C$  and obtain a Riemann surface  $X$ , but they are also an essential ingredient to computing a basis of holomorphic 1-forms on  $X$ .

A major role of Puiseux series is to provide a local coordinate chart at a singular point. For singular points of the form  $a = (1 : \alpha : \beta)$  the Puiseux series expansion  $P_j$  of  $f = f(x, y)$  such that  $P_j(0) = (\alpha, \beta)$  is a coordinate chart centered at  $(x, y) = (\alpha, \beta)$ .  $P_j$  tells us how to approach and pass through  $(x, y) = (\alpha, \beta)$  on the curve. With this coordinate chart and those at other singular points of  $C$  we can desingularize the curve and thus create an appropriate atlas for the corresponding Riemann surface  $X$ .

For the purposes of computing the genus of  $X$  as well as the space of holomorphic 1-forms  $\Gamma(X, \Omega_X^1)$  on  $X$  we need to compute the delta invariant and the multiplicity of a singularity, respectively. The following discussion assumes the singularity is finite. To analyze infinite singular points we project the curve  $C$  onto the line at infinity  $l_\infty$  using the method described in Section 2.3.

**Branching number.** The branching number  $R$  of a singular point  $(\alpha, \beta)$  is the sum of the branch numbers of the Puiseux series expansions centered at  $(x, y) = (\alpha, \beta)$ . That is,

$$R = \sum_{\substack{j \\ P_j(0)=(\alpha, \beta)}} |e_j|.$$

**Multiplicity.** As given in Section 2.3, the multiplicity of a singular point is the degree of the lowest degree non-zero homogeneous term appearing in the polynomial expression for the curve centered at  $(\alpha, \beta)$ .

**Delta invariant.** The delta invariant  $\delta_P$  of a singularity  $P$  is the number of double points concentrated at the singularity. This is equal to the number of quadratic factors  $(\alpha_i x - \beta_i y)^2$  appearing in the tangent cone at the singularity. Let  $S$  be the set of all singular points, finite and infinity, of  $C$ . Then the genus is given by

$$g = \frac{(d-1)(d-2)}{2} - \sum_{P \in S} \delta_P. \quad (3.1)$$

### Algorithm

First we determine the finite singularities of  $C : f(x, y) = 0$ . Let  $R(x)$  be the resultant of  $f(x, y)$  and  $\partial_y f(x, y)$  [10]. We compute the roots

$$\begin{aligned} S &= \{x \in \mathbb{C} \mid R(x) = 0, \partial_x R(x) = 0\} \\ &= \{x_1, \dots, x_s\}. \end{aligned}$$

For each  $x_j \in S$  we compute the  $y$ -roots  $\{y_{j1}, \dots, y_{jd}\}$  where  $d = \deg_y f$ . The places  $(x_j, y_{jk})$ ,  $j = 1, \dots, s$ ,  $k = 1, \dots, d$  satisfy

$$f(x_j, y_{jk}) = 0, \quad \partial_y f(x_j, y_{jk}) = 0,$$

by the definition of the resolvent. Therefore, the singular places  $(x_k, y_{jk})$  are those that satisfy

$$\partial_x f(x_j, y_{jk}) = 0.$$

By definition, these remaining places are the finite singular points of the curve  $C$ . For the infinite case we use the projection of the curve on the line at infinity. (See Section 2.3.)

The methods used to compute the branching number, multiplicity, and delta invariant of a singularity rely on examining the leading order behavior of the Puiseux series expansions such that  $P_j(0) = (\alpha, \beta)$ . For the details of these methods see [5]. In brief the branching number  $R$  of singularity is computed using the above formula

$$R = \sum_{P_j(0)=(\alpha, \beta)}^j |e_j|.$$

The multiplicity is the sum of the minimum of  $e_j$  and  $n_{jN}$  over all Puiseux series  $P_j$  such that  $P_j(0) = (\alpha, \beta)$  where  $\beta_{jN} t^{n_{jN}}$  is the first non-zero, non-constant term appearing in  $y_j$ . The delta invariant is equal to

$$\delta = \frac{1}{2} \sum_{j=1}^m r_j \text{Int}_{P_j} - r_j + 1,$$

where

$$\text{Int}_{P_j} = \sum_{k=1^d, k \neq j} \text{val}_x(y_j(x) - \tilde{y}_k(x)),$$

with  $\text{val}_x(g(x))$  equal to the lowest exponent of  $x$  appearing in  $g(x)$ , and  $y_j(x)$  is the  $y$ -part of  $P_j$  when solving for  $t = t(x)$ . The sum appearing in  $\text{Int}_{P_j}$  is taken over *all* Puiseux series expansions  $P_k$  at  $x = \alpha$ , not just the ones with  $P_k(0) = (\alpha, \beta)$ .

### Examples

We compute the finite singularities  $a = (1 : \alpha : \beta)$  and the infinite singularities  $a = (0 : 1 : \gamma)$  of the curve

$$C : f(x, y) = y^3 + 2x^3y - x^7 = 0.$$

```

1 from abelfunctions import *
2 from sympy.abc import x,y
3
4 f = y**3 + 2*x**3*y - x**7
5 S = singularities(f,x,y)
6
7 for s,(m,delta,r) in S:
8     if s[0] == 0:
9         print 'Infinite Singularity at:', s
10    else
11        print 'Finite Singularity at: ', s
12        print ' multiplicity      =', m
13        print ' delta invariant   =', delta
14        print ' branching number =', r
15        print

```

```

Finite Singularity at:  (1, 0, 0)
multiplicity      = 3
delta invariant   = 4
branching number = 2

```

```

Infinite Singularity at: (0, 1, 0)
multiplicity      = 4
delta invariant   = 9
branching number = 1

```

The genus is computed using the `genus()` function which, in addition to using the genus formula in Equation (??), performs additional checks on the genus using algebraic and geometric properties discussed below.

```

16 d = 7 # the homogenous degree of f is 7
17 g = (d-1)*(d-2)/2
18
19 for s,(m,delta,r) in S:

```

```

20     g -= delta
21
22     print 'degree      =', d
23     print 'genus       =', g
24     print 'genus(f,x,y) =', singularities.genus(f,x,y)

```

---

```

degree      = 7
genus       = 2
genus(f,x,y) = 2

```

### 3.3 Holomorphic 1-Forms

#### Theory

1-forms on a Riemann surface  $X$  are objects that can be integrated along piecewise smooth paths on  $X$ .

**Definition 3.3. (1-Form)** *Let  $X$  be a Riemann surface with atlas  $\{(U_\alpha, z_\alpha)\}$ . A 1-form  $\omega$  on  $X$ , also called a differential, is such that in each local coordinate  $z_\alpha : U_\alpha \subset X \rightarrow \mathbb{C}$ ,*

$$\omega \Big|_{U_\alpha} = f_\alpha(z_\alpha) dz_\alpha,$$

*and the appropriate compatibility conditions are satisfied under the action of transition functions on  $U_\alpha \cup U_\beta$  where  $(U_\beta, z_\beta)$  is another local coordinate. The space of all 1-forms on  $X$  is denoted  $\Omega_X^1$ .*

The space of all *holomorphic 1-forms* is of particular interest.

**Definition 3.4. (Holomorphic 1-Forms)** *The space of holomorphic 1-forms  $\Gamma(X, \Omega_X^1)$  on  $X$  is the space of 1-forms  $\omega$  such that in each local coordinate  $(U_\alpha, z_\alpha)$ ,*

$$\omega \Big|_{U_\alpha} = h_\alpha(z_\alpha) dz_\alpha$$

*where  $h_\alpha : U_\alpha \rightarrow \mathbb{C}$  is a holomorphic function.*

For a compact genus  $g$  Riemann surface  $X$ ,  $\Gamma(X, \Omega_X^1)$  is a finite-dimensional vector space of dimension  $g$  over  $\mathbb{C}$ . Thus, it has a basis of  $g$  holomorphic 1-forms  $\{\omega_1, \dots, \omega_g\}$ .

For Riemann surfaces obtained by desingularizing and compactifying an algebraic curve  $C : f(x, y) = 0$  these basis holomorphic 1-forms can be written as

$$\omega_k(x, y) = \frac{p_k(x, y)}{\partial_y f(x, y)} dx,$$

where  $p_k \in \mathbb{C}[x, y]$  is of degree at most  $d-3$  in  $x$  and  $y$ . The polynomials  $p_k$  are called the *adjoint polynomials of  $f$* . Note that since  $y$  has explicit dependence on  $x$  due to the equation  $f(x, y) = 0$ , we can use  $x$  as the local coordinate of the differential.

## Algorithm

One condition on the  $p_k$ 's is immediately apparent: to preserve holomorphicity  $p_k$  must have a zero, with sufficient multiplicity, at the places  $P = (\alpha, \beta)$  where  $\partial_y f(x, y)$  vanishes. More precisely, Noether showed that if a singular place  $P$  has multiplicity  $m_P$  then  $P_k$  must have a zero of order at least  $m_P - 1$  at  $P$  [19].

The technique we use to determine the adjoint polynomials  $p_k$  uses a theorem of Mñuk relying on computing an integral basis for the algebraic function field of the curve [15]. Let  $A(C)$  be the *coordinate ring*

$$A(C) = \mathbb{C}[x, y]/(f)$$

of the curve  $C : f(x, y) = 0$ . The coordinate ring can be thought of as the ring of all functions  $g \in \mathbb{C}[x, y]$  vanishing on the curve  $f$ . Note that  $A(C)$  is a subset of the *algebraic function field*  $\mathbb{C}(x, y)$ .

Given a ring  $R$  and a field  $S$  such that  $R \subset S$ , the *integral closure*  $\bar{R}$  of  $R$  in  $S$  is the ring of all elements  $s \in S$  such that

$$s^n + r_{n-1}s^{n-1} + \cdots + r_1s + r_0 = 0,$$

for some choice of  $n > 0$  and  $r_0, \dots, r_{n-1} \in R$ . That is  $\bar{R}$  consists of all elements in  $S$  satisfying some monic polynomial equation with coefficients in  $R$ . Here, we consider the integral closure  $\overline{A(C)}$  of  $A(C)$  in  $\mathbb{C}(x, y)$ .

Again, we wish to find the set of all adjoint polynomials of  $C$ . By [15], these are the set of all  $p \in \mathbb{C}[x, y]$  such that

$$\overline{A(C)}p(x, y) \subset \mathbb{C}[x, y].$$

That is, all of the polynomials  $p$  such that every element of  $\overline{A(C)}$ , when multiplied by  $p$  and reduced modulo  $f(x, y)$ , results in a polynomial. Now,  $\overline{A(C)}$  is a finite extension of  $A(C)$ . Therefore,

$$\overline{A(C)} = \beta_1 A(C) + \cdots + \beta_m A(C), \quad \beta_k \in \mathbb{C}(x, y).$$

for an appropriate choice of  $\beta_k$ 's in  $\mathbb{C}(x, y)$ . The set  $\{\beta_1, \dots, \beta_m\}$  is called the *integral basis* of the integral closure of the coordinate ring. Thus, finding the set of adjoint polynomials is equivalent to finding polynomials  $p \in \mathbb{C}[x, y]$  such that

$$\beta_k(x, y)p(x, y) \in \mathbb{C}[x, y], \quad \forall j = 1, \dots, m.$$

To compute the adjoint polynomials we write

$$p(x, y) = \sum_{i+j \leq d-3} c_{ij} x^i y^j$$

where  $d = \deg_y f$ . We compute an integral basis  $\{\beta_1, \dots, \beta_m\}$  for  $\overline{A(C)}$  using the algorithm of van Hoeij [30]. The requirement that

$$\beta_k(x, y) \sum_{i+j \leq d-3} c_{ij} x^i y^j \in \mathbb{C}[x, y]$$

imposes a number of conditions on the coefficients  $c_{ij}$  appearing in the expression for  $p(x, y)$ . The set of all possible  $c_{ij}$ 's satisfying these conditions for every  $\beta_k, k = 1, \dots, m$  gives us the adjoint polynomials we need.

## Examples

We compute a basis of holomorphic 1-forms on the Riemann surface  $X$  given by the desingularization and compactification of the algebraic curve

$$C : f(x, y) = y^3 + 2x^3y - x^7 = 0.$$

```

1 from sympy.abc import x,y,t
2
3 f = y**3 + 2*x**3*y - x**7
4 X = RiemannSurface(f,x,y)
5 oneforms = X.holomorphic_differentials()
6
7 for omega in oneforms:
8     print 'omega(x,y) =\n'
9     sympy.pprint(omega, use_unicode=False)
10    print

```

```
omega(x,y) =
```

```

      x*y
-----
      3      2
2*x  + 3*y

```

```
omega(x,y) =
```

```

      3
      x
-----
      3      2
2*x  + 3*y

```

From this we can infer that the adjoint polynomials of the curve are  $p_1(x, y) = xy$  and  $p_2(x, y) = x^3$ .

## 3.4 Analytic Continuation

### Theory

A *path on a Riemann surface* is a continuous map  $\gamma : [0, 1] \rightarrow C \subset \mathbb{C}^2$ . That is, if  $\gamma(t) = (x_\gamma(t), y_\gamma(t))$  then  $f(x(t), y(t)) = 0$  for all  $t \in [0, 1]$ . The roots of a polynomial are continuous as a function of the coefficients. Therefore, an  $x$ -path  $x_\gamma : [0, 1] \rightarrow \mathbb{C}_x$  and an initial  $y$ -root  $y_0 \in \mathbb{C}_y$  are sufficient for defining

a path on  $C$  for the resulting  $y$ -path  $y_\gamma : [0, 1] \rightarrow \mathbb{C}_y$  is completely determined by the curve

$$f(x_\gamma(t), y) = 0.$$

The process of deriving this  $y$ -path from the data provided is referred to as *analytic continuation*.

A *closed path*  $\gamma$  on a Riemann surface is one such that  $\gamma(0) = \gamma(1)$ . That is, a path is closed when  $x_\gamma(0) = x_\gamma(1)$  and  $y_\gamma(0) = y_\gamma(1)$ . When constructing a path using an  $x$ -path it may be the case that the  $x$ -path  $x_\gamma(t)$  is closed in  $\mathbb{C}_x$  but the derived  $y$ -path  $y_\gamma(t)$  may not satisfy  $y_\gamma(0) = y_\gamma(1)$ . This situation is described in more detail in Section 3.5 on monodromy groups of algebraic curves.

### Algorithm

To compute a path  $\gamma$  on a Riemann surface  $C$  we provide a continuous  $x$ -path  $x_\gamma(t)$  and an initial  $y$ -value  $y_0$  as input and we wish to receive the resulting  $y$ -path  $y_\gamma(t)$  as output. Analytic continuation of  $y_0$  along  $\gamma$  is a fundamental operation in `abelfunctions` since evaluation of and integration along paths is done frequently. Therefore, it is important to make the construction and evaluation along paths as fast and efficient as possible.

We use numerical methods to estimate values along  $y_\gamma(t)$ . In general, the problem is phrased as given  $\gamma(t_i) = (x_i, y_i)$  as well as some later  $t_{i+1} = t_i + \Delta t$  and  $x_{i+1} = x_\gamma(t_{i+1})$  determine the value  $y_{i+1} = y_\gamma(t_{i+1})$ .

A first and natural approach to solving this problem is to use a root finder. Given  $x_{i+1}$  we numerically or symbolically solve the equation

$$f(x_{i+1}, y) = 0.$$

This produces  $n$   $y$ -roots  $y_{i+1,1}, \dots, y_{i+1,d}$  over  $x_{i+1}$ . However, even if one finds an effective and fast method for doing this with arbitrary degree polynomials  $f$ , the main problem with this approach is determining which  $y_{i+1,k}$  is equal to the desired root  $y_{i+1}$ . One could argue that the desired root is the one minimizing  $|y_{i+1,k} - y_i|$  (the root closest to the previous  $y$ -root) but it is conceivable that this closest can change as a function of  $\Delta t$ , especially if  $\Delta t$  is too large.

Another approach could be to use Newton iteration: given  $x_{i+1}$  and an *initial guess*  $y_i$  at  $x_i$  use Newton iteration on the function  $g(y) = f(x_{i+1}, y)$  to determine  $y_{i+1}$ . However, this approach suffers from the same problem, namely, the root  $y_{i+1,k}$  produced by Newton iteration may change as a function of  $\Delta t$ . Too large of a  $\Delta t$  may result in *branch jumping*, where we converge to the incorrect  $y$ -root. Too small of a  $\Delta t$  gives an inefficient numerical algorithm. Further, the definition of “small enough” may change as a function of the curve  $C$  and the  $x$ -points  $x_i$  and  $x_{i+1}$ .

To solve the problem of selecting an appropriate  $\Delta t$  we use Smale’s  $\alpha$ -theory [14]. The purpose of Smale’s  $\alpha$ -theory is to answer the following questions about  $g(y) = f(x_{i+1}, y)$  for some finite set of points  $Y \subset \mathbb{C}$ :

1. From which points in  $Y$  will Newton's method converge quadratically to some solution to  $g$ ?
2. From which points in  $Y$  will Newton's method converge quadratically to distinct solutions to  $g$ ?
3. If  $g$  is real ( $\bar{g} = g$ ), from which points of  $Y$  will Newton's method converge quadratically to real solutions to  $g$ ?

See [11] for an excellent summary of Smale's  $\alpha$ -theory. Using the notation of Hauenstein and Sottile, we outline the analytic continuation algorithm here.

1. Assume we know the  $y$ -fibre  $y_i = \{y_{i,1}, \dots, y_{i,d}\}$  of  $g_i(y) := f(x_i, y) = 0$ . Fix some initial  $\Delta t$  and let  $x_{i+1} = x_\gamma(t_i + \Delta t)$ . We wish to compute the  $y$ -fibre  $y_{i+1}$  of  $g_{i+1}(y) := f(x_{i+1}, y)$  such that each element  $y_{i+1,j}$  is the analytic continuation of  $y_{i,j}$  to  $x_{i+1}$ .
2. We first determine if the  $y$ -fibre  $y_i$  is an *approximate solution* to  $g_{i+1}(y) = 0$ . Does each element of  $y_i$  lie in the quadratic convergence region of Newton's method on  $g_{i+1}$ ?  
If not, return to Step (1) with  $\Delta t \mapsto \Delta t/2$ .
3. Next, determine if the approximate solutions  $y_{i,j}$  will converge to distinct associated solutions  $y_{i+1,j}$ : will the approximate solutions jump branches or stay on their respective branches?  
If not, return to Step (1) with  $\Delta t \mapsto \Delta t/2$ .
4. The  $y$ -fibre satisfies the necessary conditions for Newton iteration to converge to the appropriate analytic continuations  $y_{i+1,j}$  at  $x_{i+1}$ . Newton iterate and output this solution  $y$ -fibre.

Note that this algorithm requires analytically continuing all of the  $y$ -roots along an  $x$ -path in the complex plane since we cannot determine an appropriate step size for continuing a given root without knowing the locations of the other roots. Although this impacts the performance of the algorithm since we have to perform  $d$  sets of Newton iterations at each step, Smale's  $\alpha$ -theory provides a rigorous method for determining an appropriate step size.

### 3.5 Monodromy

#### Theory

At a generic point  $x = \alpha_0 \in \mathbb{C}$  a curve  $C : f(x, y) = 0$  has  $d$  distinct ordered  $y$ -roots  $(y_0, \dots, y_{d-1})$  at  $\alpha_0$ . This collection of  $y$ -roots is sometimes called the *lift of* or the *fibre above*  $x = \alpha_0$ . However, at a point  $x = b$  where both  $f(x, y) = 0$  and  $\partial_y f(x, y) = 0$  the number of distinct roots in the lift is strictly less than  $d$ . Such a point  $x = b$  is called a *discriminant point* of  $f$ .

A *branch point*  $x = b$  is a discriminant point having the property that if one were to analytically continue an ordered fibre around some closed path encircling

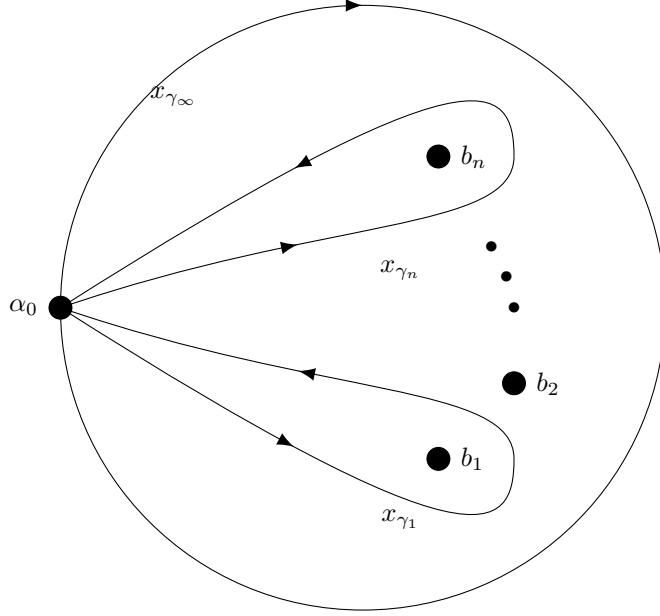


Figure 3.2: The discriminant points  $b_1, \dots, b_n$  with their respective monodromy paths  $x_{\gamma_1}, \dots, x_{\gamma_n}$  and the path  $x_{\gamma_\infty}$  around the point at infinity.

$b$  then the elements of the fibre are permuted. Specifically, let  $x_\gamma : [0, 1] \rightarrow \mathbb{C}$  be a piecewise differentiable oriented closed path in the complex  $x$ -plane encircling a branch point  $x = b$  exactly once in the positive direction and let  $(y_0, \dots, y_{d-1})$  be a fixed ordering of the fibre at  $x_\gamma(0) = b$ . Then, after analytically continuing the fibre around  $x_\gamma$  and returning to  $x_\gamma(1) = b$ , the fibre is equal to

$$(y_{\pi_b(0)}, \dots, y_{\pi_b(d-1)}),$$

where  $\pi_b \in S_d$  is a permutation on  $d$  elements. In other words, a *branch point* is a discriminant point with  $\pi_b \neq \text{id}$ .

To analyze the permutation behavior of multiple branch points  $\{b_1, \dots, b_n\}$  we start by fixing some *base point*  $x = \alpha_0$  in the complex plane such that  $\alpha_0$  is not a branch point and we fix an ordering  $(y_0, \dots, y_{d-1})$  of the fibre above  $\alpha_0$ . Let  $x_{\gamma_k} : [0, 1] \rightarrow \mathbb{C}$  be a path encircling only the branch point  $b_k$  in the positive direction which does not cross the other paths. Such a path is called a *monodromy path* of  $b_k$ . In the case when  $x = \infty$  is a branch point a monodromy path for  $\infty$  is taken to be a circle going around all of the finite branch points in the negative direction. See Figure 3.2 for an illustration of these paths.

Analytically continuing the ordered fibre  $(y_0, \dots, y_{d-1})$  around each of the branch points results in  $n + 1$  permutations

$$\pi_{b_1}, \dots, \pi_{b_n}, \pi_\infty \in S_d$$

The group generated by these permutations is called the *fundamental group* of

$\mathbb{C} \setminus \{b_1, \dots, b_n\}$ . It is denoted  $\pi_1(\mathbb{P}^1 \mathbb{C} \setminus \{b_1, \dots, b_n\}, \alpha_0)$ . Observe that, by the disjoint path condition on the monodromy paths, moving the base point  $\alpha_0$  corresponds to conjugation of the generators of the fundamental group by some  $\pi \in S_d$ . Hence, the monodromy group has explicit dependence on the base point.

### Algorithm

The algorithm implemented in `abelfunctions` for computing the monodromy group of a curve is based on the one described in [9]. Due to the technical nature of the algorithm only a summary is provided here.

- We require that the monodromy paths constructed stay sufficiently far from the branch points due to the numerical accuracy of Newton's method when used in the analytic continuation process. For each branch point,  $b_i$  we let

$$\rho_i = \min_{\substack{j=1, \dots, n \\ j \neq i}} |b_i - b_j|.$$

The minimal distance that any path  $x_\gamma$  be from the branch point  $b_i$  is

$$R_i = \frac{\rho_i \kappa}{2}$$

where  $\kappa \in (0, 1]$  is a chosen relaxation factor. The implementation of this algorithm in `abelfunctions` uses  $\kappa = 3/5$ .

- Let  $b = b_i$  be the branch point where  $\operatorname{Re} b_i < \operatorname{Re} b_j$  for all  $j \neq i$ . The point  $b$  is referred to as the *base branch point*. Choose the base point  $\alpha_0$  to be the point  $\alpha_0 = b - R_b$ , the point on the minimal distance circle encircling  $b$ .
- Order the remaining branch points  $\{b_j\}_{j \neq i}$  by increasing argument with  $b$ . This ordering determines the ordering of the monodromy paths  $x_{\gamma_j}$ .
- Construct a complete graph  $G$  with the branch points  $b_1, \dots, b_n$  as nodes and compute the minimal spanning tree  $T$  of this graph with  $b$  as the parent node.
- Using line segments and semi-circles, construct the path  $x_{\gamma_j}$  encircling  $b_j$  once in the positive direction by starting at the base point, following the minimal spanning tree to  $b_j$  and using semicircles to traverse over or under the branch points along the way depending on the ordering. That is, the path  $x_{\gamma_j}$  should be constructed in such a way so that the branch points  $b_1, \dots, b_{j-1}$  lie below the path.
- Fix an ordering of the base fibre  $(y_0, \dots, y_{d-1})$  above  $\alpha_0$  and analytically continue around each  $x_{\gamma_j}$  to determine the permutations  $\pi_j$ .

## Examples

We compute the monodromy group of the curve

$$C : f(x, y) = y^3 + 2x^3y - x^7 = 0,$$

where the permutations  $\pi_j \in \pi_1(\mathbb{P}^1\mathbb{C} \setminus \{b_1, \dots, b_n\}, \alpha_0)$  are presented in disjoint cycle notation.

```

1  from abelfunctions import *
2  from sympy.abc import x,y,t
3
4  f = y**3 + 2*x**3*y - x**7
5  X = RiemannSurface(f,x,y)
6
7  b = X.branch_points()
8  pi_1 = X.monodromy_group()
9
10 for bj,pi_1j in zip(b,pi_1):
11     print 'branch point:', bj
12     print 'permutation: ', pi_1j
13     print

```

```

branch point: (-0.31969776999-0.983928563571j)
permutation: [(0, 2), (1,)]

branch point: (0.836979627962-0.608101294789j)
permutation: [(0,), (1, 2)]

branch point: (-1.03456371594+0j)
permutation: [(0,), (1, 2)]

branch point: 0j
permutation: [(0, 2), (1,)]

branch point: (0.836979627962+0.608101294789j)
permutation: [(0,), (1, 2)]

branch point: (-0.31969776999+0.983928563571j)
permutation: [(0, 1), (2,)]

branch point: oo
permutation: [(0, 2, 1)]

```

The method `RiemannSurface.show_paths()` plots all the monodromy paths  $x_{\gamma_j}$  in the complex  $x$ -plane. The base point  $x = \alpha_0$  is marked in red.

```

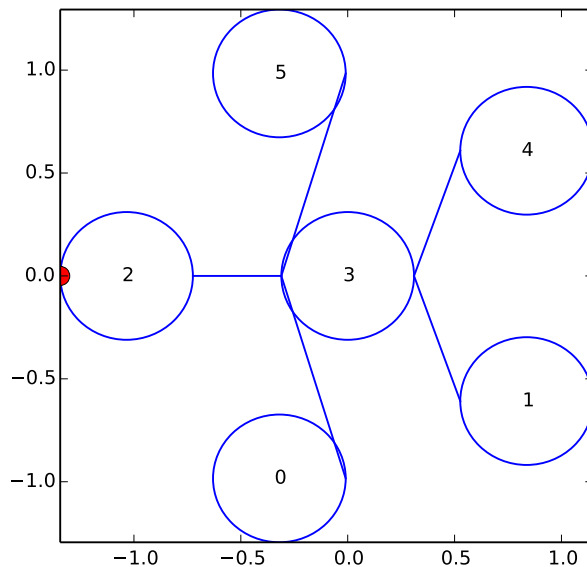
14 X.show_paths()

```

```

<matplotlib.figure.Figure object at 0x107d60810>

```



### 3.6 Homology

#### Theory

A compact Riemann surface  $X$  of genus  $g$  is homeomorphic to a sphere with  $g$  handles or, equivalently, a doughnut with  $g$  holes. A cycle on  $X$  is a closed, oriented, piecewise smooth curve  $\gamma : [0, 1] \rightarrow X$  such that  $\gamma(0) = \gamma(1)$ . The first homology group  $H_1(X, \mathbb{Z})$  of  $X$  is the collection of all cycles on  $X$  modulo homologous transformations. In this document we do not state precisely what it means for two cycles to be homologous since it involves presenting the basic theory of simplicial complexes which is beyond the scope of this document.

However, in brief, two cycles on  $X$  are homologous if they can be deformed to each other where the process of deformation not only allows continuous transformations but the splitting of one cycle into two via “pinching”. A demonstration of this procedure is shown in Figure 3.3. Two cycles can be added together by “reversing” the pinching process and negation of a path corresponds to reversing its orientation. The *first homology group*  $H_1(X, \mathbb{Z})$  is the set of all cycles on  $X$  with the addition operation described. The equivalence of cycles on a Riemann surface is the same as that of closed paths on the complex plane (specifically, the Riemann sphere) upon which one integrate a fixed meromorphic function  $g$ . Closed paths not encircling a pole of  $g$  are homologous to the zero path since they can be contracted to a point. The set of all paths encircling a single, given pole are all homologous to each other.

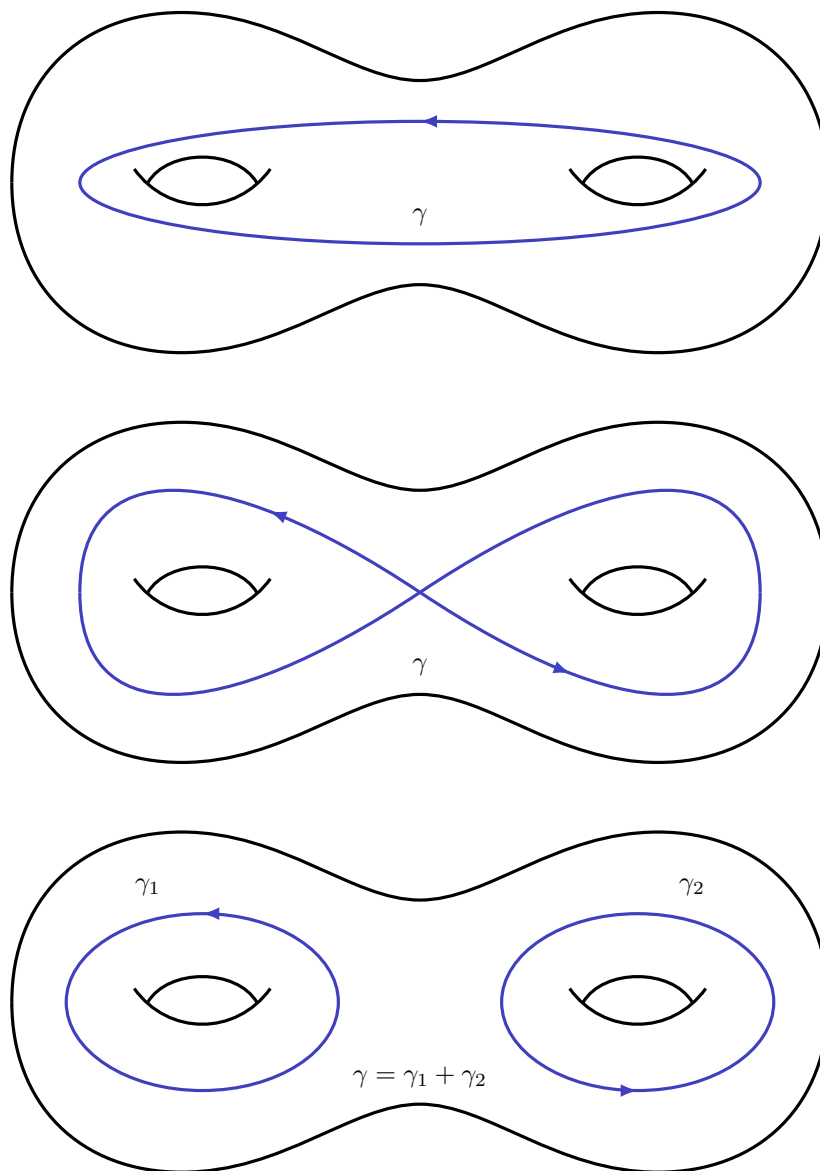


Figure 3.3: A genus  $g = 2$  Riemann surface  $X$  with three homologous cycles. The process of “pinching” and separating a cycle  $\gamma$  into two cycle is allowed. Cycles can be added together by reversing this pinching process. Negation of a cycle corresponds to reversing its orientation.

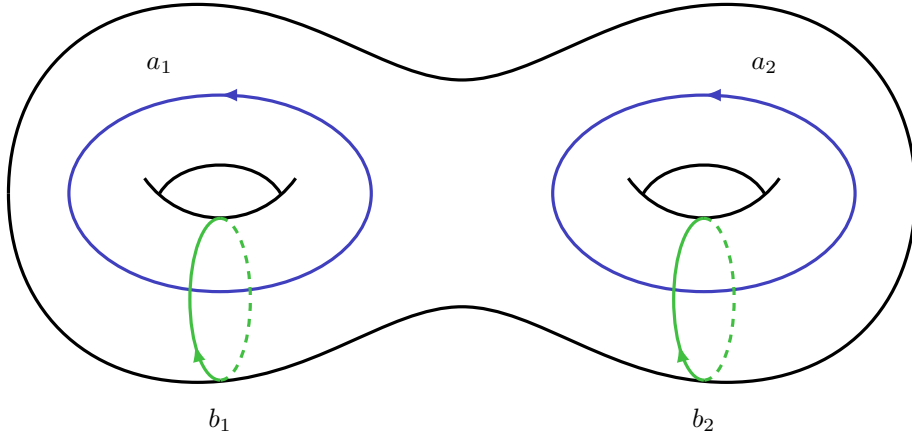


Figure 3.4: A genus  $g = 2$  Riemann surface  $X$  with the basis cycles  $\{a_1, a_2, b_1, b_2\}$  for the first homology group  $H_1(X, \mathbb{Z})$ .

$H_1(X, \mathbb{Z})$  has a basis of cycles  $\{a_1, \dots, a_g, b_1, \dots, b_g\}$ . That is, every cycle on  $X$  can be written as a finite, integer linear combination of the  $a$ - and  $b$ -cycles. These cycles can be chosen such that they satisfy the intersection properties

$$\begin{aligned} a_i \circ a_j &= 0, & \forall i \neq j \\ b_i \circ b_j &= 0, & \forall i \neq j \\ a_i \circ b_j &= \delta_{ij}, & \forall i, j = 1, \dots, g \end{aligned}$$

where  $\delta_{ij}$  is the Kronecker delta. That is, the only cycles that intersect are  $a_i$  and  $b_i$ . A basis of cycles fulfilling these intersection requirements is called a *canonical basis of cycles*. Figure 3.4 illustrates the canonical basis for a genus two Riemann surface.

### Algorithm

Tretkoff and Tretkoff [28] provide an algorithm for determining a canonical cycle basis for  $H_1(X, \mathbb{Z})$  given the monodromy group of a curve. We omit the details of the algorithm here. At its core, it computes a graph which encodes how to travel from the *base place* of  $X$ , chosen to be

$$P_0 = (\alpha_0, \beta_0)$$

where  $\alpha_0$  is the base point of the monodromy group of the curve and  $\beta_0 = y_0$  is a fixed root lying above  $x = \alpha_0$ , to the other places  $(\alpha_0, y_i)$  lying above  $x = \alpha_0$  via traversal around one or more branch points. (These places are sometimes called the *sheets* of the surface  $X$  with the  $i$ th sheet referring to the place  $(\alpha_0, y_i)$ ). A minimal spanning tree of this graph is computed where each removed edge corresponds to a cycle in  $H_1(X, \mathbb{Z})$ . This is because the addition of an edge to

the minimal spanning tree forms a cycle in the graph. This graph cycle in turn represents a possibly a non-zero cycle on  $X$ . A separate part of the algorithm is then used to compute a canonical basis of cycles by taking appropriate linear combinations of these intermediate cycles.

## Examples

We compute a homology basis for the Riemann surface  $X$  obtained by desingularizing and compactifying the curve

$$C : f(x, y) = y^3 + 2x^3y - x^7 = 0.$$

The  $a$ - and  $b$ - cycles are presented as a list  $[\dots, s_i, (b_i, r_i), s_{i+1}, \dots]$  where  $s_i$  is the current sheet number,  $b_i$  is a branch point of  $C$ ,  $r_i \in \mathbb{Z}$ , and  $s_{i+1}$  the sheet reached after rotating  $r_i$  times around  $b_i$  and returning to the base point  $\alpha_0$ .

```

1 from abelfunctions import *
2 from sympy.abc import x,y,t
3
4 f = y**3 + 2*x**3*y - x**7
5 X = RiemannSurface(f,x,y)
6 a,b = X.homology()
7
8 # print the a-cycles
9 for i in range(g):
10     print 'a_%d:'%(i+1)
11     print a[i]
12     print
13
14 # print the b-cycles
15 for i in range(g):
16     print 'b_%d:'%(i+1)
17     print b[i]
18     print

```

```

a_1:
[0, ((-0.31969776999025984-0.9839285635706635j), 1), 2,
((-1.0345637159435732+0j), -1), 1,
((-0.31969776999025984+0.9839285635706635j), -1), 0]

a_2:
[0, (0j, 1), 2, ((-0.31969776999025984-0.9839285635706635j), -1), 0]

b_1:
[0, ((-0.31969776999025984+0.9839285635706635j), 1), 1,
((0.8369796279620464-0.6081012947885316j), 1), 2,
((-0.31969776999025984-0.9839285635706635j), -1), 0]

```

```

b_2:
[0, ((-0.31969776999025984-0.9839285635706635j), 1), 2,
((-1.0345637159435732+0j), -1), 1,
((-0.31969776999025984+0.9839285635706635j), -1), 0, (oo, 1), 2,
((-0.31969776999025984-0.9839285635706635j), -1), 0,
((-0.31969776999025984+0.9839285635706635j), 1), 1,
((0.8369796279620464-0.6081012947885316j), 1), 2,
((-0.31969776999025984-0.9839285635706635j), -1), 0]

```

We can plot the projection of the cycle in the complex  $x$ - and  $y$ -planes. In this example, we plot the cycle  $a_1$  by computing 512 interpolating points on the path. The  $x$ -projection  $x_\gamma$  is in blue and the  $y$ -projection  $y_\gamma$  is in green.

```

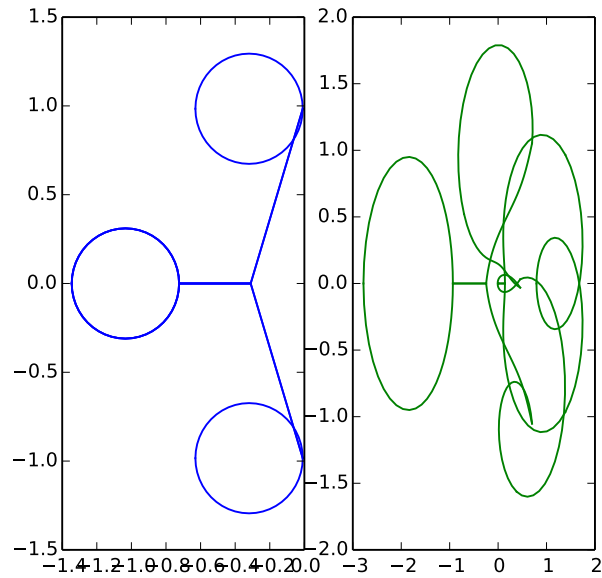
1 alpha = X.base_point()
2 betas = X.base_lift()
3 P0 = alpha, betas
4
5 gamma = RiemannSurfacePath((f,x,y), P0, cycle = a[0])
6 gamma.plot(512)

```

```

<matplotlib.figure.Figure at 0x106e9cd90>

```



### 3.7 Period Matrices

#### Theory

Period matrices are matrices obtained by integrating the holomorphic differentials  $\omega_1, \dots, \omega_g$  along the  $a$ -cycles  $a_1, \dots, a_g$  and  $b$ -cycles  $b_1, \dots, b_g$ . Define the  $g \times g$  matrices

$$A = (A_{ij})_{i,j=1}^g, \quad A_{ij} = \oint_{a_j} \omega_i,$$

$$B = (B_{ij})_{i,j=1}^g, \quad B_{ij} = \oint_{b_j} \omega_i.$$

A *period matrix* of  $X$  is the  $g \times 2g$  matrix

$$\tau = [A \ B].$$

We often normalize the differentials  $\omega_i$  such that  $A_{ij} = \delta_{ij}$  which results in the period matrix

$$\tau = [I_{g \times g} \ \Omega]. \quad (3.2)$$

This is equivalent to setting  $\Omega = A^{-1}B$ . The matrix  $\Omega \in \mathbb{C}^{g \times g}$  is a *Riemann matrix*: an invertible, symmetric complex matrix with positive definite imaginary part. The columns of  $\tau$  define a lattice

$$\Lambda = \{Im + \Omega n \mid m, n \in \mathbb{Z}^g\} \subset \mathbb{C}^g.$$

This lattice plays an important role in the theory of algebraic curves since the quotient space

$$J(C) = \mathbb{C}^g / \Lambda \cong \mathbb{T}^{2g} \quad (3.3)$$

is the *Jacobian* or *Jacobian variety* of the curve  $C$ . Jacobian varieties play a central role in the theory of algebraic curves. For example, the Torelli theorem [18] states that a non-singular projective curve is completely determined by its Jacobian. The Schottky problem establishes a link between the Jacobian and the Kadomtsev–Petviashvili equation by providing conditions on when a given Riemann matrix is a period matrix of some algebraic curve.

#### Algorithm

To compute  $A_{ij}, B_{ij}$  we first find a method for numerically integrating holomorphic differentials over any given path  $\gamma \subset C$ . We only consider finite paths on the curve: paths with finite  $x$ - and  $y$ -components. Any such path can be parameterized by some parameter  $t \in [0, 1]$ . Let

$$\gamma : [0, 1] \rightarrow C, \quad \gamma(t) = (x_\gamma(t), y_\gamma(x_\gamma(t))).$$

(Recall that we treat  $y$  as the dependent variable in  $f(x, y) = 0$ .) Given this parameterization, we compute the integral of a holomorphic differential  $\omega$ . Letting

$x$  and  $y$  represent the local coordinates in  $\mathbb{C}^2$  we have

$$\begin{aligned}\int_{\gamma} \omega &= \int_{\gamma} \omega(x, y(x)) dx \\ &= \int_0^1 \omega(x_{\gamma}(t), y_{\gamma}(x_{\gamma}(t))) \frac{dx_{\gamma}}{dt}(t) dt.\end{aligned}\tag{3.4}$$

In `abelfunctions` we construct paths  $\gamma \subset C$  where  $x_{\gamma}$  either parameterizes a line from some  $z_0 \in \mathbb{C}$  to  $z_1 \in \mathbb{C}$

$$x_{\gamma}(t) = z_0(1 - t) + z_1 t,$$

or arcs on a circle of radius  $R$  with center  $w \in \mathbb{C}$

$$x_{\gamma}(t) = w + Re^{i(\theta + t\Delta\theta)}$$

where  $\theta$  is the starting angle and  $\theta + \Delta\theta$  is the ending angle on the circle. We use the analytic continuation methods described in Section 3.4 to compute  $y_{\gamma}(x_{\gamma}(t))$ . Finally, to compute the integral in Equation (3.4) we use a numerical integrator of choice. `abelfunctions` allows one to use any numerical integrator provided by the `scipy` Python package that can integrate complex-valued functions. The Romberg method [1] is chosen by default.

## Examples

The `RiemannSurface.period_matrix()` method returns the matrices  $A$  and  $B$  defined above. The Riemann matrix  $\Omega$  is obtained by computing  $\Omega = A^{-1}B$

```

1 from abelfunctions import *
2 from sympy.abc import x,y,t
3 from scipy import dot
4 from scipy.linalg import inv
5
6 f = -x**7 + 2*x**3*y + y**3
7 X = RiemannSurface(f, x, y)
8 A,B = X.period_matrix()
9 Omega = dot(inv(A), B)
10
11 print 'A =\n', A
12 print 'B =\n', B
13 print 'Omega =\n', Omega

```

---

```

A =
[[ -1.38142275e-12-1.20192474j   1.84957199e+00+0.60096237j]
 [  9.22903420e-12+1.97146395j   7.16176201e-01-0.98573197j]]
B =
[[-0.70647363+2.17430227j -1.84957199+2.54571744j]
 [-1.87497364-1.36224808j -0.71617620+0.23269975j]]
Omega =
[[-1.30901699+0.95105652j -0.80901699+0.58778525j]
 [-0.80901699+0.58778525j -1.00000000+1.1755705j ]]

```

We numerically verify that  $\Omega$  is a Riemann matrix by computing  $\|\Omega - \Omega^T\|$  as well as the eigenvalues of  $\text{Im } \Omega$ .

14 15 16	<pre>print norm(Omega.T - Omega) print print eigvals(Omega.imag)</pre>
	<pre>9.303308740879998e-11  [ 0.46490467  1.66172235]</pre>

## 4 Future Work

The software library `abelfunctions` provides a collection of tools for computing on Riemann surfaces. Although more features need to be added most of the package's functionality is ready to be used to solve problems. In this section, I present several problems that I wish to address for my thesis:

- Provide solutions to non-linear, integrable, partial differential equations.
- Provide a framework for constructing and computing rational functions on Riemann surfaces with prescribed poles and zeros.
- Efficiently compute linear matrix representations of plane algebraic curves.

### 4.1 Solutions to Integrable Partial Differential Equations

We return to the Kadomtsev–Petviashvili (KP) equation given in the introductory section of this document:

$$(-4u_t + 6uu_x + u_{xxx})_x + 3\sigma^2 u_{yy} = 0.$$

As mentioned, the KP equation has a large class of quasi-periodic solutions of the form

$$u(x, y, t) = 2\partial_x^2 \log \theta(Ux + Vy + Wt + z_0, \Omega) + c. \quad (4.1)$$

There is a deep connection between the Riemann matrix appearing in the second argument of the theta function above and period matrices.

**Theorem 4.1. (Novikov Conjecture (1965) / Shiota Theorem (1986))**  
[27] *A Riemann matrix  $\Omega \in \mathfrak{h}_g$  is a period matrix if and only if there exists  $U, V, W, z_0 \in \mathbb{C}^g$  and  $c \in \mathbb{C}$  such that*

$$u(x, y, t) = 2\partial_x^2 \log \theta(Ux + Vy + Wt + z_0, \Omega) + c$$

*is a solution to the Kadomtsev–Petviashvili equation.*

That is, the KP equation provides a solution to the *Schottky problem*: given a Riemann matrix  $\Omega$  can we determine if it is a period matrix? In fact, as the genus  $g$  increases the likelihood that a randomly chosen Riemann matrix is a period matrix decreases. By a simple counting argument,

$$\dim_{\mathbb{C}} \mathfrak{h}_g = g(g+1)/2.$$

However,

$$\dim_{\mathbb{C}} \{\text{period matrices}\} = 3g - 3.$$

For  $g = 2, 3$  the dimensions are equal and every Riemann matrix is a period matrix. (This is also the case when  $g = 1$ .) However, for  $g > 3$  the space of Riemann matrices is larger than that of period matrices.

The main point of this discussion is that the Kadomtsev–Petviashvili equation plays a very important role in the theory of period matrices and establishes a very strong link between the fields of complex algebraic geometry and integrable partial differential equations.

It is possible to compute the constants appearing in Equation (4.1). Given a divisor  $D = \sum_i n_i P_i$  on  $X$  the parameters  $U, V, W, z_0 \in \mathbb{C}^g$  and  $c \in \mathbb{C}$  can be determined by integrating certain meromorphic differentials around certain paths on  $X$ . Deconinck [6] provides a method for determining a divisor from a set of initial data to the KP equation, thus allowing a more “physical” input to the solution algorithm. That is, the machinery for computing solutions of the form above can be used to solve the initial value problem to KP, in some sense.

The algorithms and infrastructure needed to define divisors and compute these quantities is the first problem I plan to address in my thesis work. Additionally, I will provide a standardized, programmatical framework for developers to add their own solution formulas to other integrable partial differential equations. The tools necessary for computing solutions to KP are the same as those needed to compute the parameters appearing in other finite genus solution formulas. Therefore, KP is a logical first step to this objective.

## 4.2 The Schottky–Klein Prime Form

In addition to providing the means of computing paths and 1-forms on a Riemann surface  $X$  it is important to have a way of constructing functions, other than the Abel map, defined on  $X$ . For example, is it possible to construct and subsequently compute meromorphic functions with prescribed zeros and poles on  $X$ ? That is, does a function  $E : X \times X \rightarrow \mathbb{C}$  exist such that  $E(P, Q) = 0$  if and only if  $P = Q$ ? It turns out that such a function “almost” exists yet satisfies enough properties to make the function useful.

First we need a special class of theta characteristics.

**Definition 4.2.** A non-singular odd theta characteristic  $[\delta] := [\alpha, \beta]$  is a theta characteristic where, for a given  $\alpha, \beta \in \{0, 1/2\}^g$ ,

- $\nabla \theta[\alpha, \beta](0, \Omega) \neq \mathbf{0}$  and

- $4\alpha \cdot \beta \equiv 1 \pmod{2}$ .

A **non-singular even theta characteristic** is a theta characteristic where, instead,

$$4\alpha \cdot \beta \equiv 0 \pmod{2}.$$

With these characteristics in hand, we define the function of interest.

**Definition 4.3.** *The Schottky–Klein prime form  $E : X \times X \rightarrow \mathbb{C}$  is defined by*

$$\begin{aligned} E(P, Q) &= \frac{\theta[\delta] \left( \int_P^Q \omega, \Omega \right)}{\sqrt{\zeta(P)} \sqrt{\zeta(Q)}} \\ &= \frac{\theta[\delta] (A(Q) - A(P), \Omega)}{\sqrt{\zeta(P)} \sqrt{\zeta(Q)}} \end{aligned}$$

where  $\omega = (\omega_j)_{j=1}^g$  is the vector of the normalized basis of holomorphic 1-forms of  $X$ ,  $A : X \rightarrow \mathbb{C}^g$  is the Abel–Jacobi map, and for a given non-singular odd theta characteristic  $[\delta]$

$$\begin{aligned} \zeta(P) &= \nabla \theta[\delta](0, \Omega) \cdot \omega(P) \\ &= \sum_{j=1}^g \frac{\partial}{\partial z_j} \theta[\delta](0, \Omega) \omega_j(P). \end{aligned}$$

Unfortunately,  $E$  is not holomorphic on  $X \times X$  nor is it even well defined in part because it depends on the choice of path from  $P_1$  to  $P_2$ . However, it is holomorphic and well-defined on  $\tilde{X} \times \tilde{X}$  where  $\tilde{X}$  is the universal cover of the Riemann surface  $X$  which, in this case, is the cut surface  $\hat{X}$ . The good news is that the zeros of  $E$  are independent of the choice of representative from the universal cover: if  $(\tilde{P}_1, \tilde{Q}_1) \in \tilde{X} \times \tilde{X}$  and  $(\tilde{P}_2, \tilde{Q}_2) \in \tilde{X} \times \tilde{X}$  have the same projection  $(P, Q) \in X \times X$  then  $E(\tilde{P}_1, \tilde{Q}_1) = 0$  if and only if  $E(\tilde{P}_2, \tilde{Q}_2) = 0$ .

As a result, one can use the Schottky–Klein prime form to define meromorphic functions on a Riemann surface  $X$ . Let  $P_1, \dots, P_m, Q_1, \dots, Q_n \in X$ . Then the function

$$f : X \rightarrow \mathbb{C}, \quad f(P) = \frac{\prod_{i=1}^m E(P, P_i)}{\prod_{j=1}^n E(P, Q_j)}$$

has zeros at the places  $P_1, \dots, P_m$  and poles at the places  $Q_1, \dots, Q_n$ . The ability to efficiently construct and quickly evaluate the prime form would make rational functions on Riemann surfaces as computationally accessible as Abelian functions.

### 4.3 Linear Matrix Representations

The Schottky–Klein prime form appears in the construction of linear matrix representations of certain plane curves. Every complex homogeneous polynomial in three variables can be written as

$$F(x, y, z) = \det(Ax + By + Cz)$$

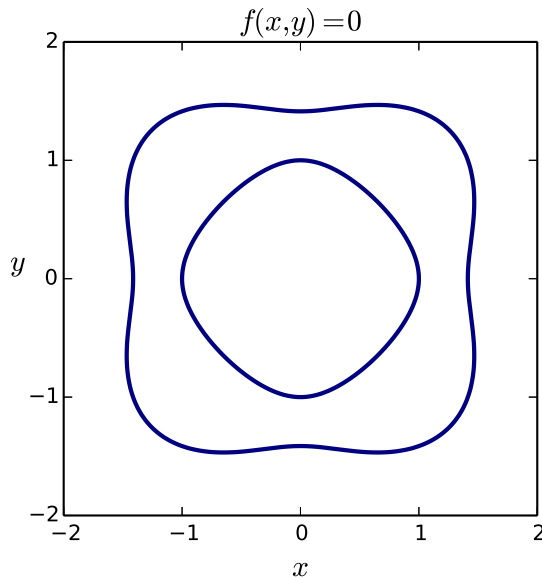


Figure 4.1: A real plot of the Helton-Vinnikov curve  $f(x, y) = x^4 + x^2y^2 - 3x^2 + y^4 - 3y^2 + 2$ . The region bounded by the innermost oval is a spectrahedron.

where  $A, B, C$  are symmetric matrices [25]. Such a representation is called a *linear matrix representation*. Linear matrix representations of polynomials appear in problems in control theory and can be used to solve polynomial inequalities via semi-definite programming [12, 21].

The curves we consider here originate from spectrahedra. A *two-dimensional spectrahedron* is a subset of  $\mathbb{R}^2$  bounded by rigidly convex algebraic curves; real curves with a maximal number of nested ovals in the real plane. The interior of the innermost oval of such a curve defines a spectrahedron. For example, the real projective curve

$$F(x_0, x_1, x_2) = 2x_0^4 + x_1^4 + x_2^4 - 3x_0^2x_1^2 - 3x_0^2x_2^2 + x_1^2x_2^2,$$

of degree four with affine part

$$f(x, y) = x^4 + x^2y^2 - 3x^2 + y^4 - 3y^2 + 2,$$

has  $4/2 = 2$  nested ovals, as shown in Figure 4.1. These curves are called *Helton-Vinnikov curves* and, by the Helton-Vinnikov theorem, completely characterize all two-dimensional spectrahedra [12].

In some applications, it is preferred to have the matrices  $A, B, C$  be real when the curve  $F$  is real. The representations important to studying spectrahedra also require that the linear matrix representation is a *real definite representation*; that is, that the span of  $A, B$ , and  $C$  contain a real positive definite matrix.

Plaumann, Sturmfels, and Vinzant [21] study several approaches to computing real definite matrices of Helton–Vinnikov curves.

The approach chosen by Helton and Vinnikov gives a positive definite linear matrix representation of a Helton–Vinnikov curve in terms of theta functions and the Schottky–Klein prime form.

**Theorem 4.4. (Helton–Vinnikov)** *Let  $C : f(x, y, z) = 0$  be a real homogeneous curve of degree  $d$  with  $f(1, 0, 0) = 0$  and assume*

1.  *$C$  is a Helton–Vinnikov curve with the point  $f(1, 0, 0) = 0$  inside the innermost oval,*
2. *the  $d$  real intersection points with the line  $\{z = 0\}$  are distinct non-singular points  $Q_1, \dots, Q_d$  with coordinates  $Q_i = (-\beta_i : 1 : 0)$ ,  $\beta_i \neq 0$ ,*
3.  *$\delta$  is an even theta characteristic with  $\theta[\delta](0, \Omega) \neq 0$ .*

Then,

$$f(x, y, z) = \det(Ix + By + Cz),$$

where  $I$  is the  $d \times d$  identity matrix,  $B = \text{diag}(\beta_1, \dots, \beta_d)$ , and  $C$  is a real symmetric matrix with diagonal entries

$$c_{ii} = \beta_i \frac{\partial_z f(-\beta_i, 1, 0)}{\partial_y f(-\beta_i, 1, 0)},$$

and off-diagonal entries

$$c_{jk} = \frac{\beta_k - \beta_j}{\theta[\delta](0, \Omega)} \frac{\theta[\delta](A(Q_k) - A(Q_j))}{E(Q_j, Q_k)},$$

where  $E : X \times X \rightarrow \mathbb{C}^g$  is the Schottky–Klein prime form.

The calculation of linear matrix representations of Helton–Vinnikov curves is an excellent application of the Schottky–Klein prime form and I aim to provide an algorithm for doing so.

#### 4.4 The Constructive Schottky Problem

As mentioned, the KP equation provides a means for determining if a Riemann matrix  $\Omega \in \mathfrak{h}_g$  comes from the period matrix of some Riemann surface  $X$ . The question can be asked, can we find a curve  $C : f(x, y) = 0$  producing this period matrix. This question is called the Constructive Schottky Problem. That is,

Given a Riemann matrix  $\Omega \in \mathfrak{h}_g$  can we find a curve  $C : f(x, y) = 0$  with  $\Omega$  as its period matrix?

This is a long-term endeavor. Regardless, I aim to examine possible avenues for addressing this problem.

## 5 Bibliography

### References

- [1] *Romberg's method*, [http://en.wikipedia.org/wiki/Romberg's\\_method](http://en.wikipedia.org/wiki/Romberg's_method), March 2014, [Online; accessed 11-March-2014].
- [2] H. F. Baker, *Abelian functions: Abel's theorem and the allied theory of theta functions*, Cambridge University Press, Cambridge, 1897.
- [3] E. Bézout, *Théorie générale des équations algébriques*, Ph.D. Pierres, University of Lausanne, 1779.
- [4] B. Deconinck, *NIST Digital Library of Mathematical Functions: Multidimensional Theta Functions*, <http://dlmf.nist.gov/21>, Release 1.0.6 of 2013-05-06, Online companion to [20].
- [5] B. Deconinck and M. Patterson, *Computing with plane algebraic curves and riemann surfaces: The algorithms of the Maple package Algcurves*, Computational Approach to Riemann Surfaces, Lecture Notes in Mathematics, Springer Berlin, Heidelberg, 2011.
- [6] B. Deconinck and H. Segur, *The kp equation with quasiperiodic initial data*, Physica D. Nonlinear Phenomena **123** (1998), no. (1-4), 12352.
- [7] B. Dubrovin, *Theta functions and non-linear equations*, Russian Math. Surveys **36** (1981), no. 2, 11–92.
- [8] D. Duval, *Rational puioux expansions*, Composito Mathematica **70** (1989), no. 2, 119–154.
- [9] J. Frauendiener, C. Klein, and V. Shramchenko, *Efficient computation of the branching structure of an algebraic curve*, Computational Methods and Function Theory **11** (2012), no. 2, 527–546.
- [10] P. A. Griffiths, *Introduction to algebraic curves*, Translations of mathematical monographs, American Mathematical Society, 1989.
- [11] J.D. Hauenstein and F. Sottile, *alphacertified: Certifying solutions to polynomial systems*, ACM Transactions on Mathematical Software (TOMS) **38** (2012), no. 4, 28.
- [12] J. W. Helton and V. Vinnikov, *Linear matrix inequality representations of sets*, Communications on Pure and Applied Mathematics **60** (2007), no. 5, 654–647.
- [13] I. Krichever, *The cauchy problem for doubly periodic solutions of kp-ii equation*, Important Developments in Soliton Theory (A.S. Fokas and V.E. Zakharov, eds.), Springer Series in Nonlinear Dynamics, Springer Berlin Heidelberg, 1993, pp. 123–146 (English).

- [14] The merging of disciplines: new directions in pure, applied, and computational mathematics (Laramie, Wyo., 1985), *Newtons method estimates from data at one point*, Springer, 1986.
- [15] M. Mñuk, *Computing adjoint curves*, J. Symb. Comput. **23** (1997), 229–240.
- [16] D. Mumford, *Tata lectures on theta i*, Modern Birkhäuser Classics, Birkhäuser, Boston, MA, 1983.
- [17] ———, *Tata lectures on theta ii*, Modern Birkhäuser Classics, Birkhäuser, Boston, MA, 1983.
- [18] David B. Mumford, *Appendix: Curves and their jacobians*, The Red Book of Varieties and Schemes, Lecture Notes in Mathematics, vol. 1358, Springer Berlin Heidelberg, 1999, pp. 225–291.
- [19] M. Noether, *Rationale ausführungen der operationen in der theorie der algebraischen funktionen*, Math. Ann. **23** (1983), 311–358.
- [20] F. W. J. Olver, D. W. Lozier, R. F. Boisvert, and C. W. Clark (eds.), *NIST Handbook of Mathematical Functions*, Cambridge University Press, New York, NY, 2010, Print companion to [4].
- [21] D. Plaumann, B. Sturmfels, and C. Vinzant, *Computing linear matrix representations of Helton–Vinnikov curves*, (preprint) (2010), <http://arxiv.org/abs/1011.6057>.
- [22] ———, *Quartic curves and their bitangents*, Journal of Symbolic Computation **46** (2011), 712–733.
- [23] J. Plucker, *Solution d’une question fondamentale concernant theorie generale des courbes*, J. Reine. Agnew. Math. **12** (1834), 105–108.
- [24] M. Pocchiola and G. Vegter, *The visibility complex*, SCG ’93 Proceedings of the ninth annual symposium on Computational geometry (1993), 328–337.
- [25] R. Quarez, *Symmetric determinantal representation of polynomials*, Linear Algebra and its Applications **436** (2012), no. 9, 3642 – 3660.
- [26] G. B. Riemann, *Zur theorie der Abelschen funktionen für den fall  $p = 3$* , (1876), 466–472.
- [27] T. Shiota, *Characterization of Jacobian varieties in terms of soliton equations*, Inventiones Mathematicae **83** (1986), no. 2, 333–382.
- [28] C. L. Tretkoff and M. D. Tretkoff, *Combinatorial group theory, riemann surfaces and differential equations*, Contemp. Math. **33** (1984), 467–517.
- [29] K. Ueno and K. Nomizu, *An introduction to algebraic geometry*, Translations of mathematical monographs, American Mathematical Society, 1997.

- [30] M. van Hoeij, *An algorithm for computing an integral basis in an algebraic function field*, J. Symb. Comput. **18** (1994), 353–363.